Trends In Carbohydrate Research Vol.16, No.4 (2024) 72-93

0975-0304/09

Trends in Carbohydrate Research

Synthesis, Antimicrobial, Antibiofilm, and SAR Studies of 6-*O*-Heptanoyl-α-D-Glucopyranoside Derivatives

Nasrin Akter[a], Imtiaj Hasan[b,c] and Sarkar M. A. Kawsar[a*]

[a]Laboratory of Carbohydrate and Nucleoside Chemistry (LCNC), Department of Chemistry, Faculty of Science, University of Chittagong, Chittagong-4331, Bangladesh

[b]Department of Biochemistry and Molecular Biology, University of Rajshahi, Rajshahi-6205, Bangladesh

[c]Department of Microbiology, University of Rajshahi, Rajshahi-6205, Bangladesh

Received: December 03, 2024; Revised and accepted: December 30, 2024

Graphical Abstract

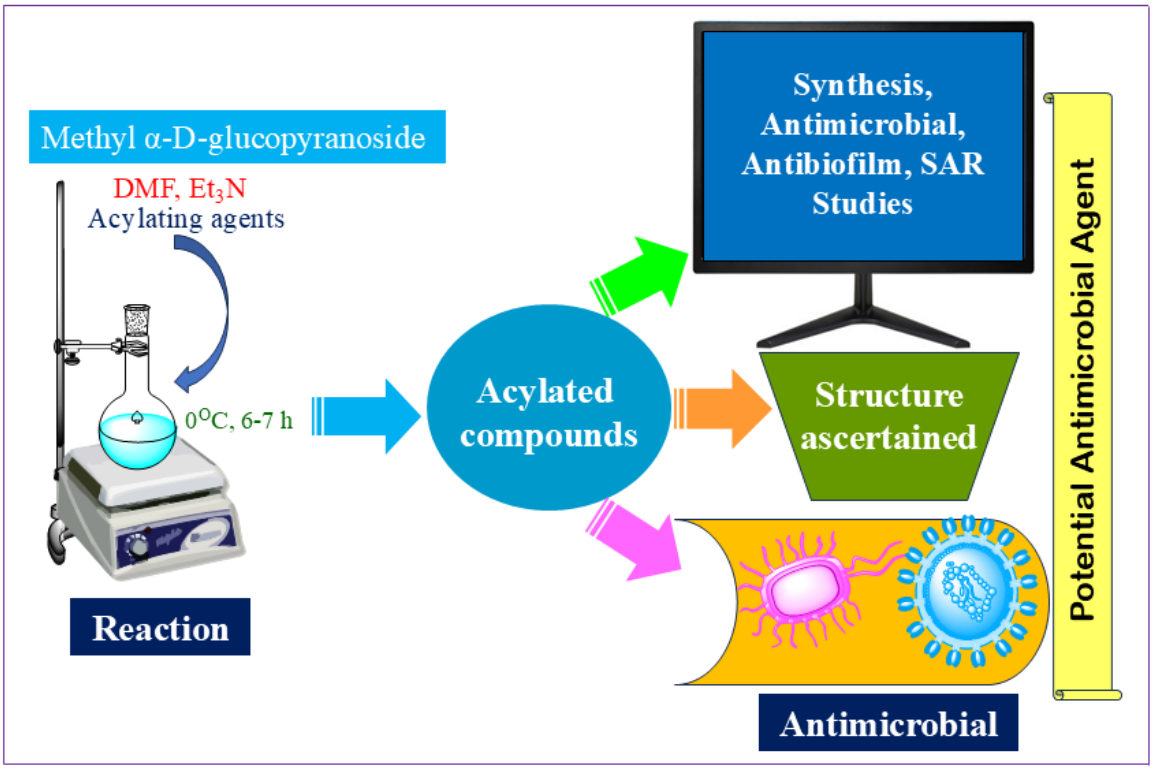

* Corresponding author: Sarkar M. A. Kawsar
E-mail: akawsarabe@yahoo.com; Tel: +88-01762717081

Abstract

Carbohydrates represent a hitherto unexplored reservoir of novel pharmaceutical compounds, thereby presenting promising prospects for therapeutic applications. From this perspective, the present study aimed to explore the synthesis and evaluation of antimicrobial activity, antibiofilm assessment and physicochemical features investigations. This work describes biologically active methyl α-D-glucopyranoside (**1**) derivatives (MGP, **2-6**) bearing aliphatic/aromatic acyl moieties, which were synthesized and analyzed *via* FTIR, $^{1}H/^{13}C$-NMR and elemental analysis. *In vitro* antimicrobial tests against five bacteria and two fungi and the prediction of activity spectra for substances (PASS) indicated promising antibacterial functionality for these glucopyranoside derivatives (**2-6**) compared with antifungal activity. The formation of biofilms by *Escherichia coli* was inhibited by a methyl 6-*O*-heptanoyl-2,3,4-tri-*O*-myristoyl-α-D-glucopyranoside derivative (**6**). The antibiofilm activities of the compounds were determined to be 8.63, 7.19, and 6.47% at concentrations of 1000, 500, and 250 µg/mL, respectively. A structure–activity relationship (SAR) investigation revealed that the myristoyl chain [$CH_3(CH_2)_{12}CO$-] and the haloaromatic chain [2-$Cl.C_6H_4CO$-] in combination with sugar had the most potent activity against bacterial and fungal pathogens.

Keywords: Synthesis; SAR; Antibiofilm; Antimicrobial; Heptanoyl-α-D-glucopyranoside

1. Introduction

Carbohydrates are essential chemicals that play important roles in almost every element of life, including the formation of genetic and energy materials, the support of organismal structure, the formation of invasion and host defense systems, and the formation of secondary antibiotic metabolites. Naturally occurring carbohydrates and their derivatives have been intensively investigated as medicinal treatments for a variety of disorders. Carbohydrates and carbohydrate-containing compounds play significant roles in practically every aspect of life.[1] Carbohydrate-based compounds,[2,3] including streptomycin, neomycin, and gentamicin, were identified as anti-infectives in the 1940s; adriamycin was found and established as a prevalent anticancer drug; ganglioside GM1 was isolated and formulated as a treatment for severe stroke; and the polysaccharide hyaluronic acid was examined for its potential in arthritis therapy.[4] Indeed, the numerous biological roles of carbohydrates establish a framework for the development of carbohydrate-based medications.[5] Glycans, a distinct type of carbohydrate, have been associated with several maladies, including cancer, inflammation, and microbial infections.[6,7] Vaccines, antiviral medicines, and immunotherapies have been developed by utilizing particular interactions between glycans and lectins.[8,9]

Several carbohydrate-based medicines are presently available for a variety of medical uses. Carbohydrates, particularly monosaccharides, have prompted researchers to investigate the relative reactivity of various hydroxyl groups at different locations. The idea of relative reactivity and a reaction sequence that reflects the dexterity of modern carbohydrate chemistry helps one to synthesize a range of physiologically and visually active natural compounds.

Modern and advanced techniques have recently been applied for the isolation of several natural chemicals from plants[10] and other sources in which carbohydrates are crucial.[11] One can also selectively acylate carbohydrates to develop new, physiologically active molecules.

Monosaccharide derivatives have a wide range of biological activities against both gram-negative and gram-positive species, including *Escherichia coli*, *Bacillus subtilis*, *Salmonella typhi*, and *Staphylococcus aureus*.[12,13] It has been shown that altering the hydroxyl group quantity in nucleoside and monosaccharide structures is a great way to make efficient antiviral[14-16] and antimicrobial[17,18] drugs. We introduced different aliphatic and aromatic acyl groups to the hydroxyl (-OH) group of methyl α-D-glucopyranoside (**1**) in our laboratory and carbohydrate moities containing FDA-approved drugs are marketed (**Figure 1**). We performed antimicrobial screening to determine the minimum inhibitory concentrations (MICs), minimum bactericidal concentrations (MBCs), and antibiofilm effects of all drugs that might have been used to determine their antibiofilm properties. This study aimed to identify possible innovations and accelerate the synthesis of new antimicrobial agents.

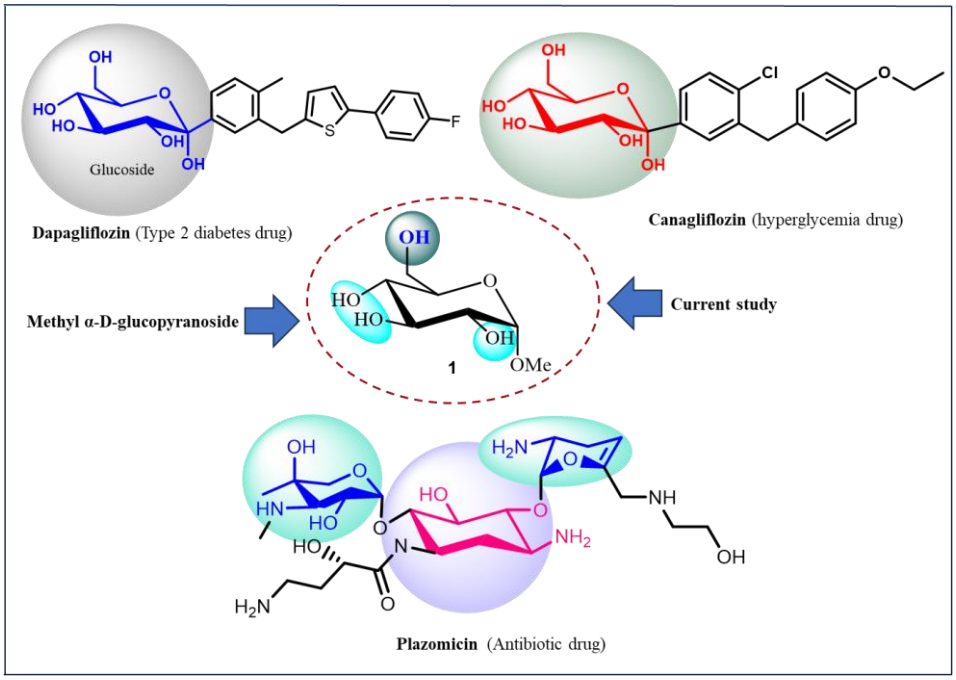

Figure 1. Carbohydrate scaffolds-containing FDA-approved drugs.

2. Experimental

2.1. Materials

Unless otherwise stated, all of the reagents used in this work were from Aldrich and were used. An engine electrothermal melting point instrument was used to determine the melting points. The values that are acquired are unchangeable. Using a Buchi rotary evaporator manufactured in West Germany, the evaporation process was conducted under decreased pressure. The bath temperature was maintained at 40 °C. For solutions in $CDCl_3$ and MeOH-d_4,

NMR spectra (400 MHz) were acquired at the BCSIR Laboratory in Dhaka. Kieselgel GF254 was the stationary phase; silica gel G_{60} was used in the column chromatography technique.

2.2. Synthesis of MGP derivatives

After cooling to -5 °C, 1.1 molar equivalents of heptanoyl chloride (0.07 mL) were added to a solution of methyl α-D-glucopyranoside (**1**, 100 mg, 0.515 mmol) in dry pyridine (10.0 mL) and continuously stirred at 0 °C for 6 hours. The mixture was stirred at room temperature all night. Analysis *via* TLC (CH_3OH-$CHCl_3$, 1:6) revealed the development of a product with a faster rate of motion (R_f = 0.52). After a few ice cubes were added to the flask to eliminate any remaining reagent, 3×10 mL of $CHCl_3$ was used to extract the contents. The mixture was allowed to settle into a saturated aq. $NaHCO_3$ solution and distilled water after the combined $CHCl_3$ layer was repeatedly washed sequentially with dilute HCl (10%). The filtrate was concentrated under low pressure after the organic layer ($MgSO_4$) was dried and filtered. To obtain the title compound (**2**, 107 mg, 85%), the resulting combination was run via silica gel column chromatographic purification (with CH_3OH-$CHCl_3$, 1:6 as the eluent). The heptanoyl derivative (**2**) from ethyl acetate-*n*-hexane was obtained as a needle from which the next stage commenced.

2.2.1. Methyl 6-*O*-heptanoyl-α-D-glucopyranoside (2)

Yield %85, m.p.: 78-79 °C, R_f = 0.53, recrystallization (EtOAc-*n*-hexane), FTIR: ν_{max} 1711 (-CO), 3401~3507 (br) (-OH) cm^{-1}. ^{1}H-NMR (400 MHz, $CDCl_3$): δ_H 5.11 (1H, d, J = 3.5 Hz, H-1), 5.07 (1H, dd, J = 2.1 and 12.1 Hz, H-6a), 4.68 (1H, dd, J = 2.2 and 12.2 Hz, H-6b), 4.28 (1H, t, J = 9.6 Hz, H-4), 4.25 (1H, t, J = 9.4 Hz, H-3), 3.92 (1H, dd, J = 3.6 and 10.1 Hz, H-2), 3.52 (1H, ddd, J = 2.8, 9.8 and 12.6 Hz, H-5), 3.50 (3H, s, 1-OC*H*$_3$), 2.38 {2H, m, $CH_3(CH_2)_4CH_2CO$-}, 1.61 {2H, m, $CH_3(CH_2)_3CH_2CH_2CO$-}, 1.30 {6H, m, $CH_3(CH_2)_3CH_2CH_2CO$-}, 0.89 {3H, m, $CH_3(CH_2)_5CO$-}. ^{13}C-NMR (100 MHz, $CDCl_3$): δ_C 174.55, 172.71, 172.75 {3×$CH_3(CH_2)_5CO$-}, 97.11 (C-1), 74.97 (C-2), 69.34 (C-4), 68.58 (C-3), 63.37 (C-5), 63.08 (C-6), 55.19 (1-O*C*H$_3$), 34.07, (×2) 34.05, 33.85, 31.22, (×2) 31.12, 24.74, (×3) 24.55, 22.25, (×2) 22.16, 21.86 {3×$CH_3(CH_2)_5CO$-}, 13.84, 13.80, 13.78 {3×$CH_3(CH_2)_5CO$-}. LC-MS $[M+1]^+$ 306.36. Calcd. for $C_{14}H_{26}O_7$: C=54.88, H=8.55; found: C= 54.90, H=8.54%.

2.2.2. General procedure for the preparation of 6-*O*-heptanoyl derivatives (3-6)

A solution of heptanoyl derivative (**2**, 115 mg, 0.29 mmol) in dry pyridine (3 mL) was cooled to -5 °C when benzoyl chloride (0.26 mL, 5 molar eq.) was added. The mixture was stirred at 0 °C for 5 h and then allowed to stand at room temperature overnight. Work-up as described earlier and chromatographic purification with CH_3OH-$CHCl_3$ (1:6) as the eluent afforded benzoyl derivative **3** (218 mg, 79%) as a colorless crystalline solid.

2.2.3. Methyl 6-*O*-heptanoyl-2,3,4-tri-*O*-benzoyl-α-D-glucopyranoside (3)

A solution of heptanoyl derivative (**2**, 115 mg, 0.29 mmol) in dry pyridine (3 mL) was cooled to -5 °C when benzoyl chloride (0.26 mL, 5 molar eq.) was added. The mixture was stirred at 0 °C for 5 h and then allowed to stand at room temperature overnight. Work-up as

described earlier and chromatographic purification with CH_3OH-$CHCl_3$ (1:6) as the eluent afforded benzoyl derivative **3** (218 mg, 79%) as a colorless crystalline solid.

Yield %79, m.p.: 88-89 °C, R_f = 0.52, recrystallization (EtOAc-*n*-hexane), FTIR: ν_{max} 1708 (-CO) cm^{-1}. ^{1}H-NMR (400 MHz, $CDCl_3$): δ_H 8.11 (6H, m, 3×Ar-H), 7.60 (3H, m, 3×Ar-H), 7.45 (6H, m, 3×Ar-H), 5.31 (1H, d, J = 3.5 Hz, H-1), 5.02 (1H, d, J = 3.5 Hz, H-2), 4.92 (1H, dd, J = 3.4 and 9.2 Hz, H-3), 4.90 (1H, t, J = 9.3 Hz, H-4), 4.10 (1H, dd, J = 5.0 and 12.0 Hz, H-6a), 3.86 (1H, m, H-6b), 3.64 (1H, m, H-5), 3.41 (3H, s, 1-OC*H*$_3$), 3.04 {2H, m, $CH_3(CH_2)_4CH_2CO$-}, 1.66 {2H, m, $CH_3(CH_2)_3CH_2CH_2CO$-}, 1.36 {6H, m, $CH_3(CH_2)_3CH_2CH_2CO$-}, 0.89 {3H, m, $CH_3(CH_2)_5CO$-}. ^{13}C-NMR (100 MHz, $CDCl_3$): δ_C 175.55, 174.71, 173.75 {3×$CH_3(CH_2)_5CO$-}, 164.60, 164.58, 164.53 (3×C_6H_5CO-), 133.11, 133.08, (×2) 133.01, 129.95, (×3) 129.88, 129.85, (×2) 129.77, (×3) 128.79, (×2) 127.86, (×2) 127.38 (3×C_6H_5CO-), 97.11 (C-1), 72.97 (C-2), 71.34 (C-4), 70.58 (C-3), 69.37 (C-5), 63.08 (C-6), 55.19 (1-O*C*H$_3$), 34.07, (×2) 34.05, 33.85, 31.22, (×2) 31.12, 24.74, (×3) 24.55, 22.25, (×2) 22.16, 21.86 {3×$CH_3(CH_2)_5CO$-}, 13.84, 13.80, 13.78 {3×$CH_3(CH_2)_5CO$-}. LC-MS $[M+1]^+$ 618.72. Calcd. for $C_{35}H_{38}O_{10}$: C=67.79, H=6.18; found: C= 67.81, H=6.19%.

Similar reaction and purification methods were employed to synthesize 2-chlorobenzoyl (**4**) (190.15 mg) as a crystalline solid), 2-bromobenzoyl (**5**) (192.20 mg) as a solid), and myristoyl (**6**) (190 mg as a crystalline solid) derivatives.

2.2.4. Methyl 2,3,4-tri-*O*-(2-chlorobenzoyl)-6-*O*-heptanoyl-α-D-glucopyranoside (4)

Yield %77.31, m.p.: 105-106 °C, R_f = 0.55, recrystallization (EtOAc-*n*-hexane), FTIR: ν_{max} 1707 (-CO) cm^{-1}. ^{1}H-NMR (400 MHz, $CDCl_3$): δ_H 8.06 (3H, m, 3×Ar-H), 7.66 (6H, m, 3×Ar-H), 7.39 (3H, m, 3×Ar-H), 4.92 (1H, d, J = 3.5 Hz, H-1), 4.82 (1H, dd, J = 3.5 and 10.1 Hz, H-2), 4.71 (1H, t, J = 9.6 Hz, H-3), 4.67 (1H, m, H-4), 4.31 (1H, m, H-6a), 3.77 (1H, dd, J = 2.0 and 12.2 Hz, H-6b), 3.53 (1H, m, H-5), 3.37 (3H, s, 1-OC*H*$_3$), 2.36 {2H, m, $CH_3(CH_2)_4CH_2CO$-}, 1.67 {2H, m, $CH_3(CH_2)_3CH_2CH_2CO$-}, 1.30 {6H, m, $CH_3(CH_2)_3CH_2CH_2CO$-}, 0.92 {3H, m, $CH_3(CH_2)_5CO$-}. ^{13}C-NMR (100 MHz, $CDCl_3$): δ_C 175.58, 174.80, 173.77 {3×$CH_3(CH_2)_5CO$-}, 164.63, 164.25, 163.78 (3×2-Cl.C_6H_4CO-), 132.44, 132.38 (×3), 131.29, 130.84 (×2), 129.81 (×3), 128.93 (×2), 126.52, 126.01 (×3), 125.50, 125.11 (3×2-Cl.C_6H_4CO-), 97.14 (C-1), 72.93 (C-2), 71.37 (C-4), 70.53 (C-3), 69.36 (C-5), 63.01 (C-6), 55.13 (1-O*C*H$_3$), 34.03, (×2) 34.11, 33.87, 31.26, (×2) 31.13, 24.76, (×3) 24.56, 22.20, (×2) 22.12, 21.84 {3×$CH_3(CH_2)_5CO$-}, 13.87, 13.85, 13.72 {3×$CH_3(CH_2)_5CO$-}. LC-MS $[M+1]^+$ 722.04. Calcd. for $C_{35}H_{35}Cl_3O_{10}$: C=58.21, H=4.80; found: C= 58.22, H=4.81.

2.2.5. Methyl 2,3,4-tri-*O*-(2-bromobenzoyl)-6-*O*-heptanoyl-α-D-glucopyranoside (5)

Yield %76.45, m.p.: 75-76 °C, R_f = 0.53, recrystallization (EtOAc-*n*-hexane), FTIR: ν_{max} 1705 (-CO) cm^{-1}. ^{1}H-NMR (400 MHz, $CDCl_3$): δ_H 8.0 (3H, m, 3×Ar-H), 7.68 (6H, m, 3×Ar-H), 7.42 (3H, m, 3×Ar-H), 4.87 (1H, d, J = 3.7 Hz, H-1), 4.79 (1H, dd, J = 3.6 and 10.1 Hz, H-2), 4.68 (1H, t, J = 9.5 Hz, H-3), 4.64 (1H, m, H-4), 4.13 (1H, m, H-6a), 3.48 (1H, dd, J

= 2.1 and 12.1 Hz, H-6b), 3.44 (1H, m, H-5), 3.27 (3H, s, 1-OC*H*$_3$), 2.39 {2H, m, CH$_3$(CH$_2$)$_4$C*H*$_2$CO-}, 1.65 {2H, m, CH$_3$(CH$_2$)$_3$C*H*$_2$CH$_2$CO-}, 1.31 {6H, m, CH$_3$(C*H*$_2$)$_3$CH$_2$CH$_2$CO-}, 0.89 {3H, m, C*H*$_3$(CH$_2$)$_5$CO-}. ^{13}C-NMR (100 MHz, CDCl$_3$): δ_C 175.52, 174.65, 173.77 {3×CH$_3$(CH$_2$)$_5$*C*O-}, 164.67, 164.61, 163.80 (3×3-Br.C$_6$H$_4$*C*O-), 132.43 (×3), 132.40 (×2), 132.37 (×3), 130.97 (×3), 129.88 (×3), 126.50 (×2), 125.64 (×2) (3×3-Br.*C*$_6$H$_4$CO-), 97.09 (C-1), 72.95 (C-2), 71.36 (C-4), 70.53 (C-3), 69.32 (C-5), 63.03 (C-6), 55.17 (1-O*C*H$_3$), 34.02, (×2) 34.09, 33.88, 31.24, (×2) 31.11, 24.70, (×3) 24.53, 22.24, (×2) 22.11, 21.88 {3×CH$_3$(*C*H$_2$)$_5$CO-}, 13.86, 13.84, 13.75 {3×*C*H$_3$(CH$_2$)$_5$CO-}. LC-MS $[M+1]^+$ 855.39. Calcd. for C$_{35}$H$_{35}$Br$_3$O$_{10}$: C=49.31, H=4.12; found: C= 49.30, H=4.13%.

2.2.6. Methyl 6-*O*-heptanoyl-2,3,4-tri-*O*-myristoyl-α-D-glucopyranoside (6)

Yield %82.60, m.p.: 55-56 °C, R_f = 0.51, recrystallization (EtOAc-*n*-hexane), FTIR: ν_{max} 1707 (-CO) cm^{-1}. ^{1}H-NMR (400 MHz, CDCl$_3$): δ_H 5.30 (1H, d, J = 3.7 Hz, H-1), 4.79 (1H, dd, J = 3.5 and 10.2 Hz, H-2), 4.72 (1H, t, J = 9.8 Hz, H-3), 4.70 (1H, t, J = 9.5 Hz, H-4), 4.09 (1H, dd, J = 2.1 and 12.2 Hz, H-6b), 3.97 (1H, dd, J = 4.5 and 10.2 Hz, H-6a), 3.95 (1H, m, H-5), 3.42 (3H, s, 1-OC*H*$_3$), 2.37 {6H, m, 3×CH$_3$(CH$_2$)$_{11}$C*H*$_2$CO-}, 2.37 {2H, m, CH$_3$(CH$_2$)$_4$C*H*$_2$CO-}, 1.66 {6H, m, 3×CH$_3$(CH$_2$)$_{10}$C*H*$_2$CH$_2$CO-}, 1.65 {2H, m, CH$_3$(CH$_2$)$_3$C*H*$_2$CH$_2$CO-}, 1.27 {60H, m, 3×CH$_3$(C*H*$_2$)$_{10}$CH$_2$CH$_2$CO-}, 1.27 {6H, m, CH$_3$(C*H*$_2$)$_3$CH$_2$CH$_2$CO-}, 0.90 {9H, m, 3×C*H*$_3$(CH$_2$)$_{12}$CO-}, 0.89 {3H, m, C*H*$_3$(CH$_2$)$_5$CO-}. ^{13}C-NMR (100 MHz, CDCl$_3$): δ_C 175.49, 174.68, 173.59 {3×CH$_3$(CH$_2$)$_5$*C*O-}, 172.50, 172.45, 172.38 {3×CH$_3$(CH$_2$)$_{12}$*C*O-}, 97.08 (C-1), 72.90 (C-2), 71.31 (C-4), 70.49 (C-3), 69.38 (C-5), 63.05 (C-6), 55.13 (1-O*C*H$_3$), 34.31, 34.35, 34.11 (×2), 31.90, 31.84 (×2), 29.53 (×2), 29.40, 29.33, 29.28 (×2), 29.27 (×3), 29.18, 25.04 (×2), 24.97, 24.95, 22.68 (×3), 22.68, 22.57 (×3), 22.52 (×3), 21.70, 21.62, 20.07 (×2), 20.01 {3×CH$_3$(*C*H$_2$)$_{12}$CO-}, 34.02, (×2) 34.01, 33.82, 31.27, (×2) 31.16, 24.78, (×3) 24.54, 22.27, (×2) 22.14, 21.88 {3×CH$_3$(*C*H$_2$)$_5$CO-}, 14.09, 14.04, 14.02 {3×*C*H$_3$(CH$_2$)$_{12}$CO-}, 13.85, 13.81, 13.77 {3×*C*H$_3$(CH$_2$)$_5$CO-}. LC-MS $[M+1]^+$ 937.44. Calcd. for C$_{56}$H$_{104}$O$_{10}$: C=71.74, H=11.18; found: C= 71.75, H=11.17%.

2.3. *In vitro* antimicrobial activity

To evaluate the efficacy of antimicrobial activity, two plant pathogenic fungi and five human pathogenic bacteria were utilized. In accordance with the CLSI methodology,[19] the antibacterial susceptibility of the compounds was assessed through conventional disc diffusion experiments. The test microorganisms were selected from plates using a sterile inoculation loop and subsequently suspended in sterile normal saline (0.85%) to prepare the inoculums. The density of the suspension was determined by comparison with the McFarland 0.5 standard. The inhibition zones around the discs were measured in millimeters (mm) after the plates were incubated for an additional 18 hours at 37 °C. The trials were re-conducted.

2.4. Measurement of the MIC and MBC

Microdilution methods are preferred for measuring MIC and MBC values because they assess the concentration of the antimicrobial agent in the broth medium and quantify its antibacterial activity *in vitro*. A twofold dilution of the test chemical (0.125, 0.25, 0.5, 1, 2, 4, or 8

mg/mL) was created by dispensing 100 µL of each 2x compound mixture in column 1 of a 96-well microtiter plate containing 100 µL of MHB broth. The chemical solutions were serially diluted from columns 2-10. All the wells received 5 µL of a test strain inoculum at 104-105 CFU/mL, which was diluted from a standardized solution calibrated to the 0.5 McFarland scale, except for the sterile control well (blank). The inoculated 96-well microtiter plates were incubated at 37 °C for 24 hours. Each well received 10 mL (0.5 w/v) 2,3- and 5-triphenyl tetrazolium chloride solutions. The cultures were then incubated at 37 °C for 24 hours. The emergence of the red color signified bacterial development, and the MIC and MBC were determined visually.

2.5. Screening of mycelial growth

The poisoned food technique[20] was utilized to screen the antifungal efficacy of potato dextrose agar (PDA). After the test compounds were dissolved in 1% (w/v) dimethyl sulfoxide, 0.1 mL of the solution containing 1 mg of each was pipetted into a sterile Petri dish. After that, 20 mL of the medium was placed in a Petri plate for solidification. To inoculate each Petri dish, a 5 mm mycelium block of each fungus was placed in the center. The blocks were reversed in the center of each Petri plate to optimize mycelium–culture media contact. During the triplicate experiments, the inoculation plates were incubated at 27±2 °C. The same conditions were applied to the PDA without the test chemicals or a control sample. After five days of incubation, the diameter of fungal radial mycelial growth was measured. Three measurements were averaged to calculate the fungal radial mycelial growth in millimeters.

2.6. Antibiofilm activity

Escherichia was cultured in liquid nutrient medium at 37 °C until the optical density of the bacterial mixture at 640 nm reached 1.0. Compound 6 was serially diluted after being placed into the wells of a microtiter plate. Following the addition of the bacterial suspension to each well to a total volume of 100 µL, the plate was incubated for 48 hours at 37 °C. The bacterial cells in each well were stained with a 0.1% (w/v) solution of crystal violet (20 µL) and incubated for 15 minutes at 25 °C to identify the presence of biofilms. A micropipette was used to extract the bacterial mixture, and 100 µL of isopropanol was added to each well to eliminate the unattached crystal violet.[21] After that, the absorbance values were obtained via an automated microtiter plate reader at 640 nm. The ability of compound 6 to suppress biofilm formation was evaluated with the following formula:

% of biofilm inhibition = [absorbance of (control- test) / absorbance of control] × 100.

2.7. Structure-activity relationship (SAR)

The molecular structure of the pharmacological target was used to predict antibacterial activity using the structure–activity relationship (SAR) analysis method. This well-known technology is frequently employed to direct the synthesis or acquisition of novel compounds with desired features during the drug design process. The SAR was examined in the current work using Hunt's membrane permeation theory[22] and Kim.[23]

3. Results and Discussion

3.1. Chemistry

This work's primary goal was to apply the direct acylation[24,25] approach to methyl α-D-glucopyranoside (**1**) by selective heptanoylation (**Scheme 1**). To obtain newer derivatives of synthetic and biological significance and to gather supportive evidence for structural elucidation, these derivatives of the resulting heptanoylation products were also synthesized by employing a wide variety of acylating agents. Furthermore, the hydroxyl groups in carbohydrates must be selectively acylated to synthesize both the acylation products and biologically active natural products. As a result, the products that are produced can be used as flexible intermediates in the synthesis of numerous significant chemical compounds.

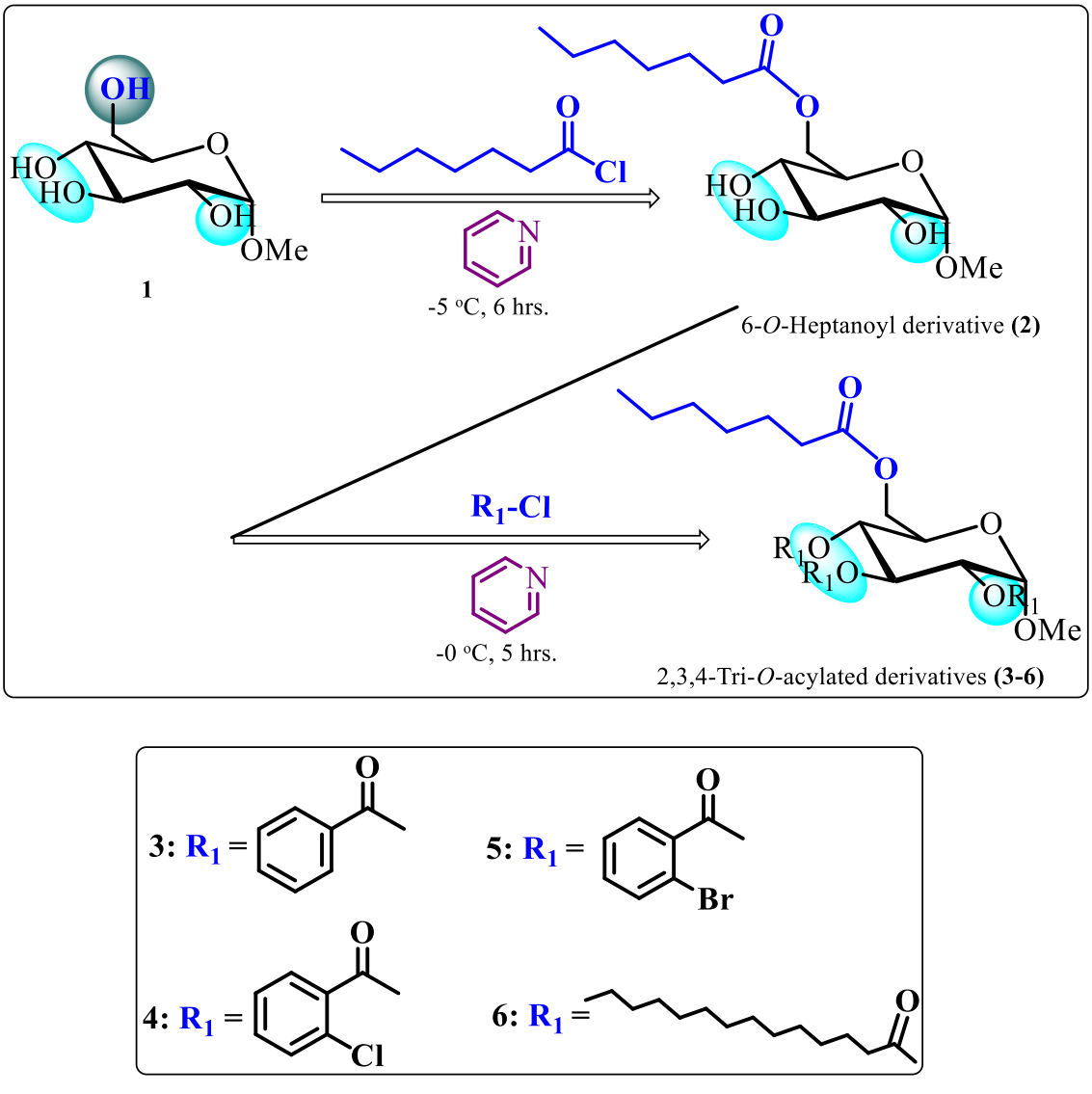

Scheme 1. Synthetic pathway of MGP derivatives with reagents and condition.

3.2 Characterization

In **Scheme 1**, methyl α-D-glucopyranoside (**1**) is treated with heptanoyl chloride in dry pyridine at -5 °C. Following the standard work-up, compound **2** was produced in excellent yield, and **Figure 2** shows the anticipated mechanism which is supported by Giri et al.[26] The following bands were observed in the FTIR spectrum (**Figure 3**) 1731 cm^{-1} for -CO stretching and 3401-3507 cm^{-1} (br, -OH) for -OH stretching. The ^{1}H-NMR spectrum (**Figure 4**) clearly revealed that a monosubstitution product had formed, which displayed peaks of two proton multiplets at δ 2.38 {$CH_3(CH_2)_4CH_2CO$-}, δ 1.61 {$CH_3(CH_2)_3CH_2CH_2CO$-}, six proton multiplets at δ 1.30 {$CH_3(CH_2)_3CH_2CH_2CO$-} and three proton multiplets at δ 0.89 {$CH_3(CH_2)_5CO$-}, corresponding to the presence of three heptanoyl groups in the molecule. The downfield shift of C-6 protons to δ 5.17 and δ 5.09 from precursor (**1**) values (~4.00 ppm)[27] and the resonances of additional protons in expected places indicate heptanoyl group attachment at position 6. The increased reactivity of the sterically less hindered primary -OH group, 1-OH>2-OH>3-OH, may yield compound (**2**). All the heptanoyl group peaks were observed in the ^{13}C-NMR spectra. Compound (**2**) was $C_{14}H_{26}O_7$ and had a molecular ion peak at m/z [M+1]+ 306.36. We proposed the structure of the substance as methyl 6-*O*-heptanoyl-α-D-glucopyranoside (**2**) after analyzing the FTIR and ^{1}H-/^{13}C-NMR spectra.

The benzoyl derivative (**3**) of the identical heptanoyl derivative **2** showed an absorption peak at 1711 cm^{-1} for carbonyl (-CO) stretching but no hydroxyl stretching in its FTIR spectrum (**Figure 4**). The 1H-NMR spectra show three benzoyl groups in the molecule, with aromatic proton peaks at δ 8.11, δ 7.60, and δ 7.45. Additionally, C-2, C-3, and C-4 resonated at δ 5.02, δ 4.92, and δ 4.90, respectively, downfield to triol (**3**) values, indicating the introduction of three lauroyl groups at positions 2, 3, and 4. FTIR ^{1}H-/^{13}C-NMR spectroscopy revealed that the benzoate structure was methyl 2,3,4-tri-*O*-benzoyl-6-*O*-(heptanoyl)-α-D-glucopyranoside (**3**).

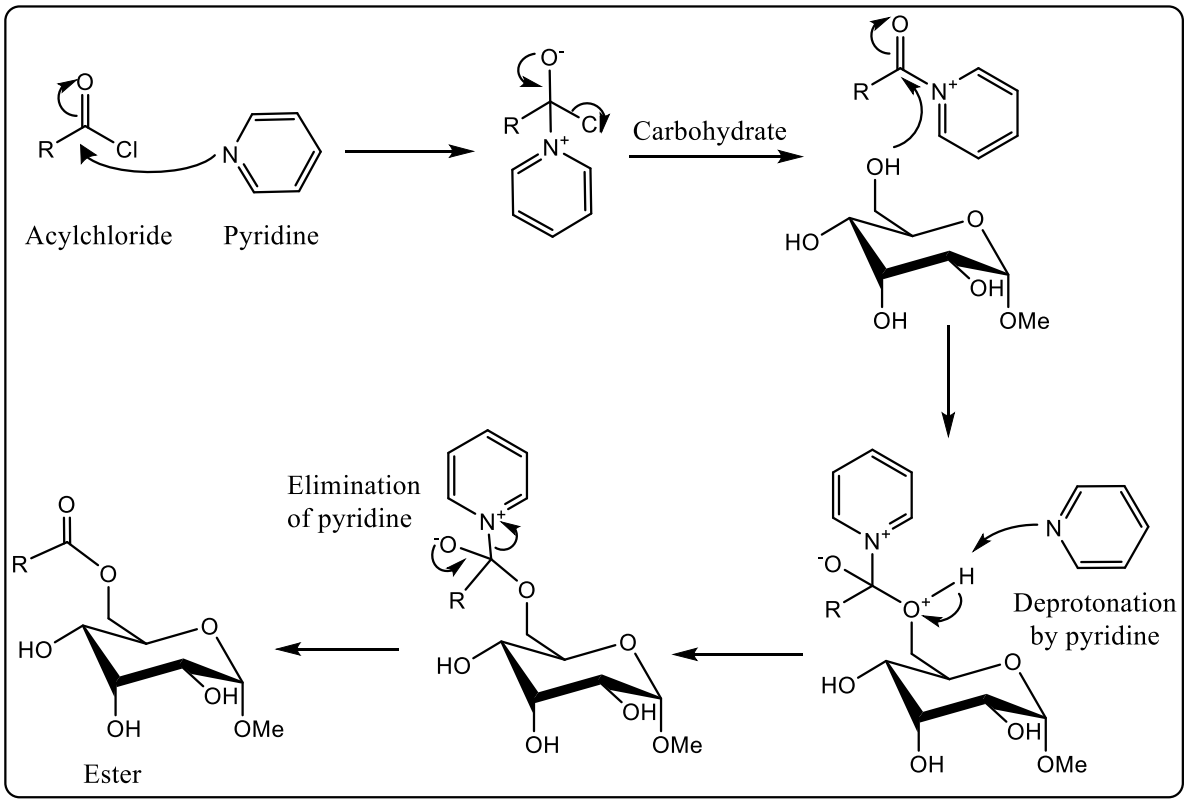

Figure 2. Expected mechanism of the acylation reaction. Here, R = alkyl- group.

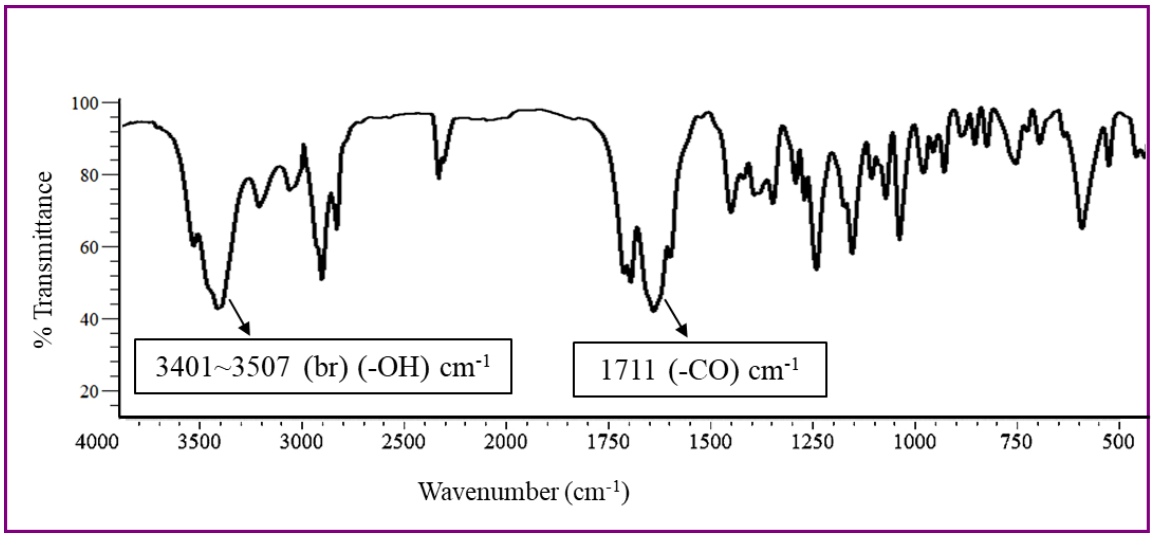

Figure 3. The FTIR spectrum of the compound **2**.

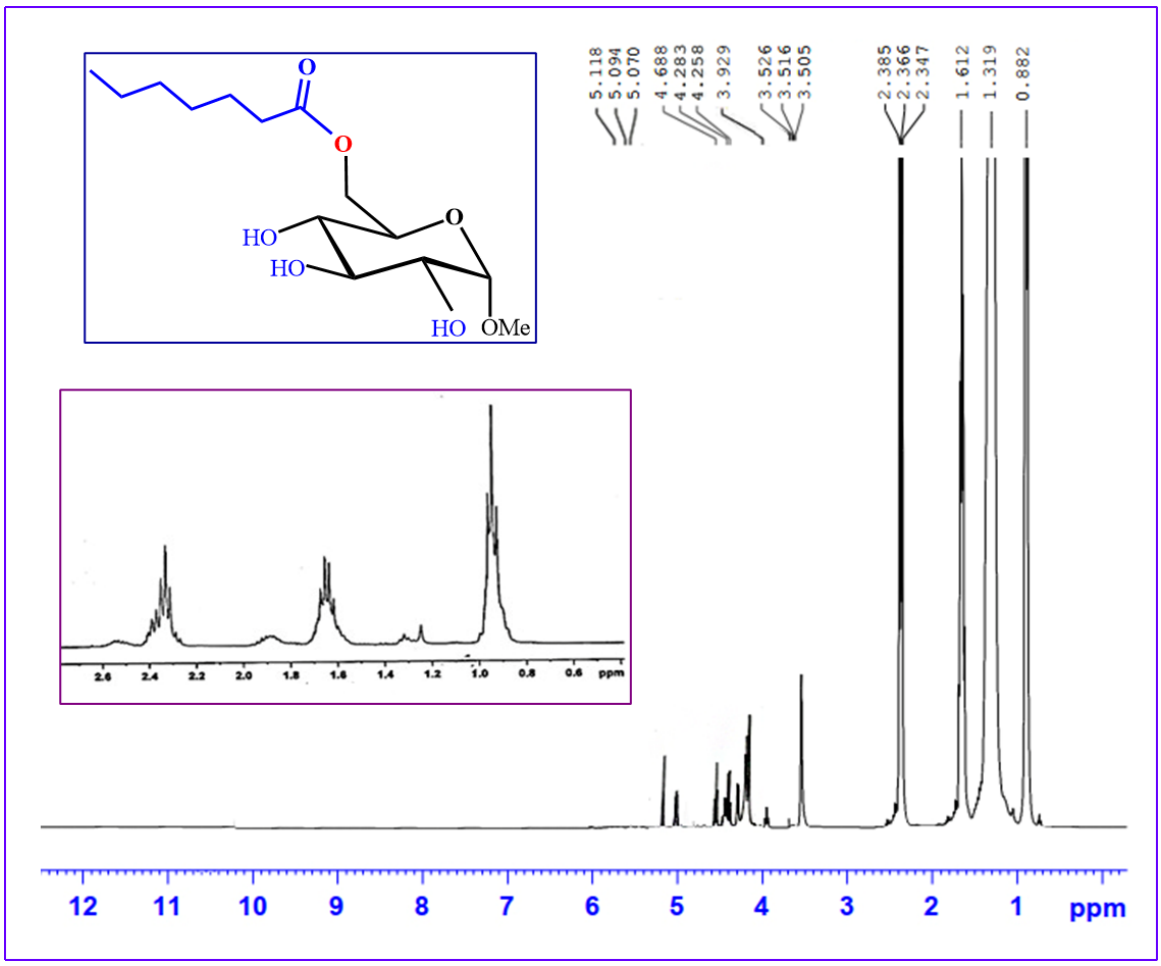

Figure 4. The ^{1}H-NMR spectrum of the compound **2**.

The tri-*O*-benzoyl derivative (**4**) was produced by reacting the heptanoyl derivative (**2**) with an equimolecular amount of 2-chlorobenzoyl chloride at freezing temperatures. This compound's FTIR spectrum (**Figure 5**) showed a carbonyl (-CO) stretching absorption peak at 1711 cm^{-1} but no hydroxyl stretching. The presence of three 2-chlorobenzoyl groups in the molecule was confirmed by the appearance of two three-proton multiplets at δ 7.80 and δ7.39 and a six-proton multiplet at δ 7.66 in its ^{1}H-NMR spectrum. For compound (**5**), bromobenzoylation of **2** with an excess of 2-bromobenzoyl chloride in anhydrous pyridine was performed, and the resulting product was subsequently purified. The ^{1}H-NMR spectrum revealed the formation of a tri-*O*-bromobenzoate product with three triplets at δ 7.88, one six-proton triplet at δ 7.68, and one triplet at δ 7.42, corresponding to the aromatic ring protons of three 2-bromobenzoyl groups in the molecule. By analyzing all the spectra, we determined the structure of the derivative to be methyl 2,3,4-tri-*O*-(2-bromobenzoyl)-6-*O*-heptanoyl-α-D-

glucopyranoside (**5**). Thus, compound **2** yielded a myristoyl derivative (**6**) after myristoyl chloride treatment. The FTIR spectra (**Figure 5**) revealed a C=O stretching absorption band at 1707 cm^{-1}. Three myristoyl groups in the molecule caused typical six-proton multiplets at δ 2.37 and δ 1.66, a sixty-proton multiplet at δ 1.27, and a nine-proton multiplet at δ 0.90 in its ^{1}H-NMR spectrum. The myristoyl derivative was identified as a methyl 6-*O*-heptanoyl-2,3,4-tri-*O*-myristoyl-α-D-glucopyranoside (**6**) after the remaining spectra and other structural features were analyzed.

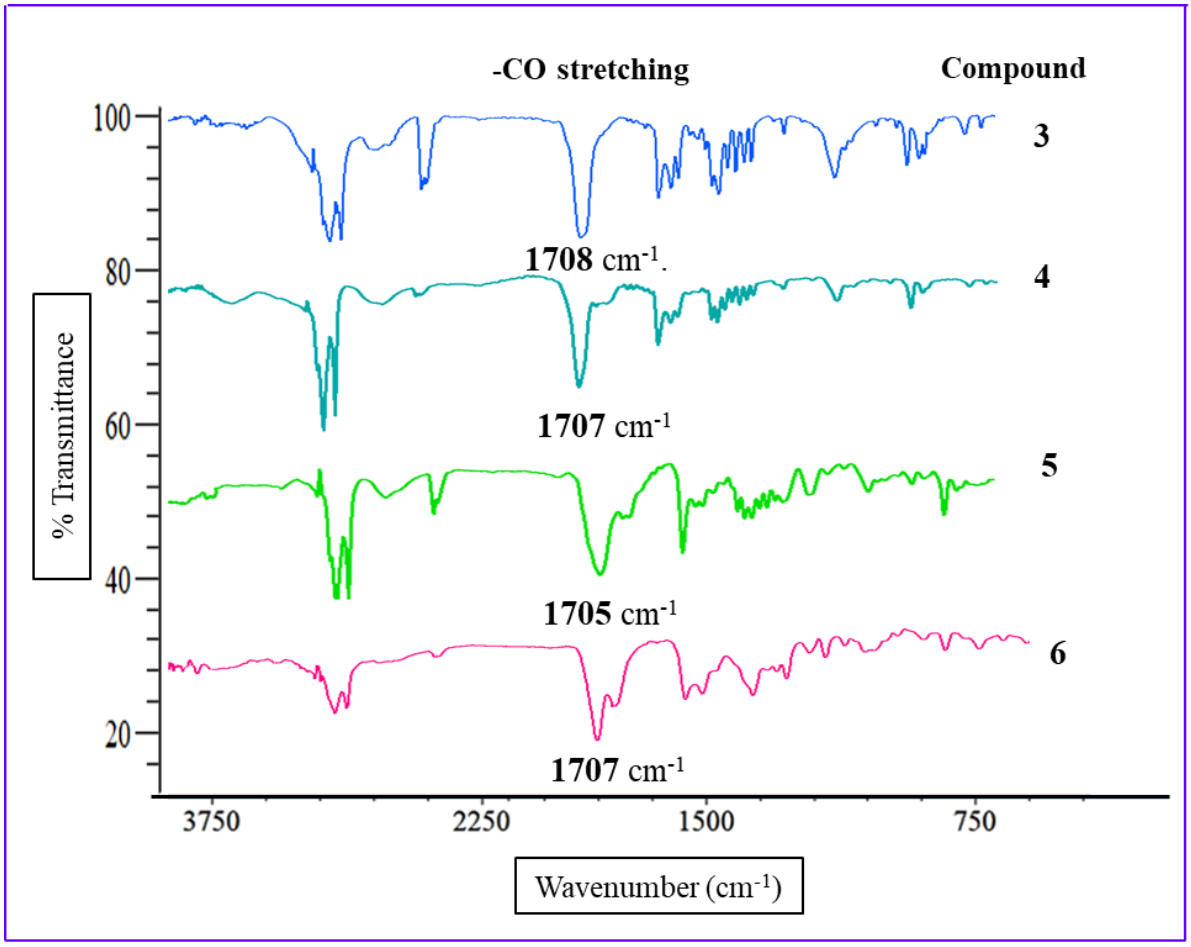

Figure 5. FTIR spectra of compounds **3-7**.

3.3 Antibacterial potential

Since carbohydrate derivatives are predicted to act at the genomic level and inhibit transcription or replication mechanisms that are essential for microbial survival, their usage can be viewed as a unique option. Since bacteria lack substitute pathways for these fundamental metabolic functions, carbohydrate derivatives that obstruct these pathways function as potent antimicrobial agents.[28] **Figure 6** displays the preliminary antibacterial activity results. The *in vitro* antibacterial efficacy of the synthesized MGP derivatives (**2–6**) was evaluated against a range of gram-

positive (**Figure 6**) and gram-negative (**Figure 7**) bacterial strains. In accordance with earlier research, the disc diffusion method and broth microdilution method were employed to determine the MIC and MBC.[29] Compound **4** exhibited a significant zone of inhibition against *Bacillus subtilis* (12.75 mm) and *Bacillus cereus* (10.75 mm), whereas compound **5** exhibited the largest zone of inhibition against both of these microbes (12.45 mm). Furthermore, compound **6** exhibited a promising zone of inhibition against the species *B. cereus* (8.00 mm) and *B. subtilis* (10.00 mm).

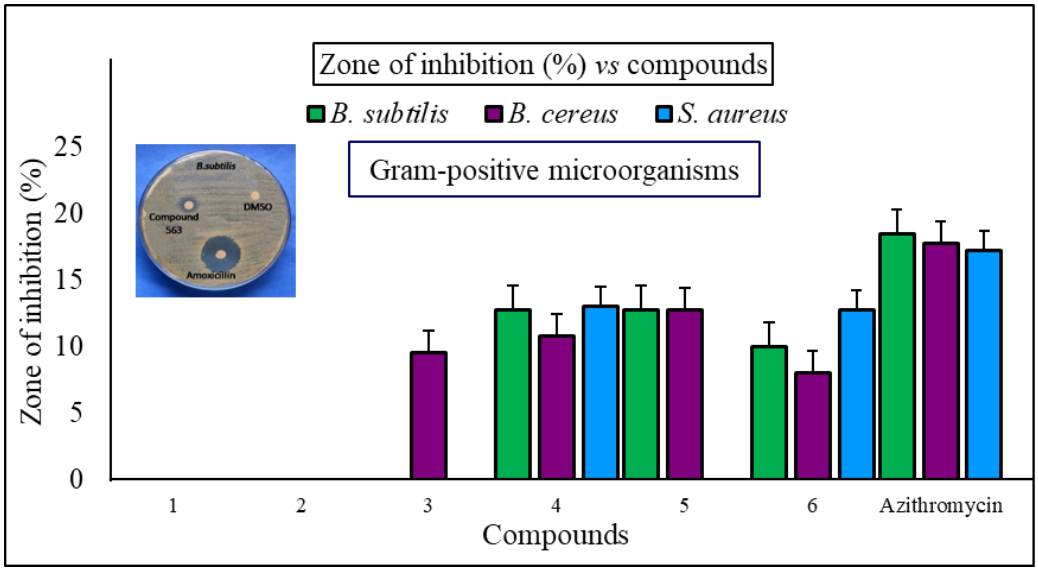

Figure 6. Compounds (**1-6**) are inhibited by the gram-positive bacteria.

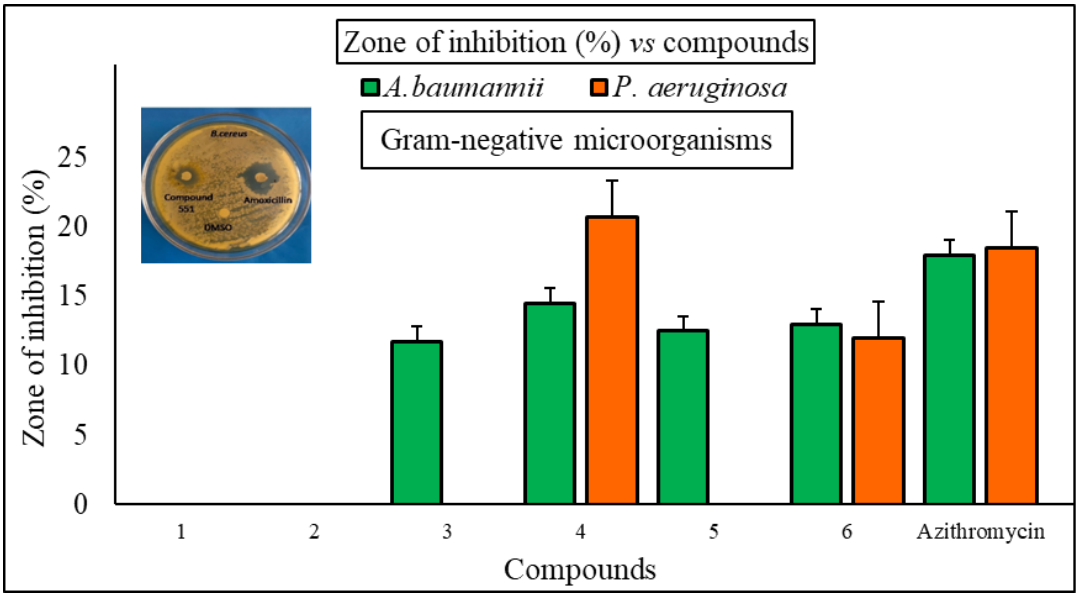

Figure 7. Compounds **1-6** are inhibited by the gram-negative bacteria.

Compounds **4** and **6** exhibited zones of inhibition for all the gram-positive and gram-negative microorganisms that were tested. In contrast, *Acinetobacter baumannii* exhibited a compound **4** (14.50 mm) zone, whereas *Pseudomonas aeruginosa* exhibited a (20.75 mm) zone of inhibition. Compound **6** demonstrated a moderate zone of inhibition against the gram-negative bacteria *A. baumannii* (13.00 mm) and *P. aeruginosa* (12.00 mm). The compounds can be arranged as **4**>**6**>**5**>**3**>**2** on the basis of this activity.

3.4 MIC and MBC evaluation

The MICs and MBCs of the most potent glucopyranoside derivatives were determined to assess their antibacterial properties against pathogenic microorganisms.[30] The results are listed in **Figures 8** and **9**. The best antibacterial effects against the tested strains were found for MGP derivatives **4** and **6**, which presented MIC values in the range of 0.125–128 mg/mL. Compounds **4** and **6** demonstrated activities against each tested bacterium, with compound **4** demonstrating the highest activity against *S. aureus* (0.125 mg/mL). Compound **6** exhibited notable efficacy against most of the test pathogens at remarkably low concentrations; *B. cereus* was the target of the highest activity, at 0.5 mg/mL. The lowest MBC values were observed for both compounds **4** and **6** against *B. subtilis* and *B. cereus*, at 8.00 mg/mL. In addition, these compounds had the highest MBC values (16.00 mg/mL) against *S. aureus*, *A. baumannii*, and *P. aeruginosa*. The MBC values of these compounds, which are capable of destroying the other tested organisms, were within the range of 8.00–16.00 mg/mL.

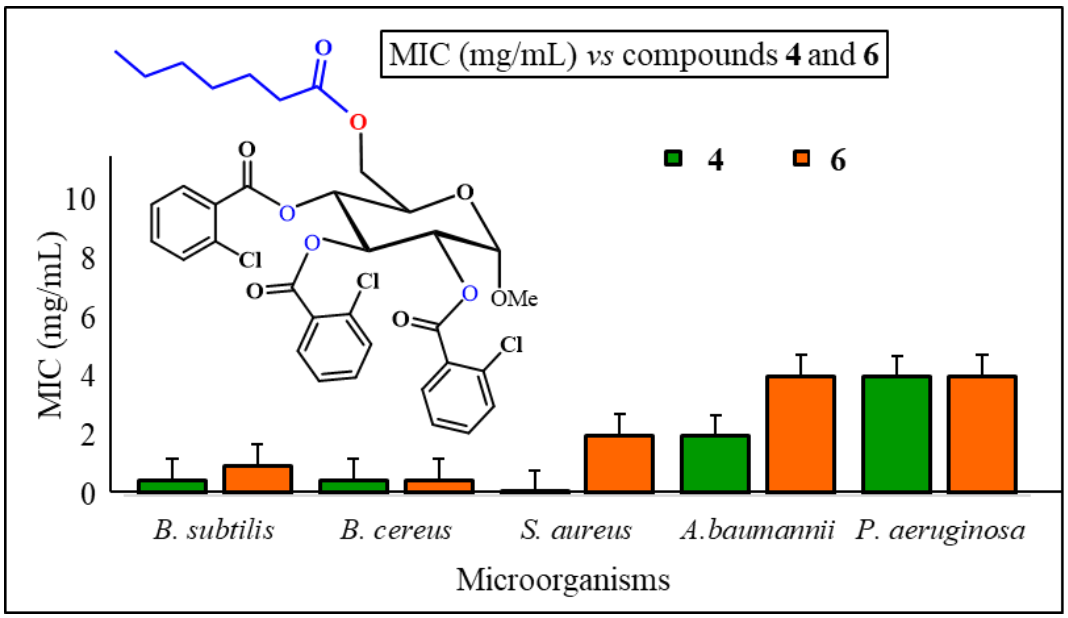

Figure 8. MIC values against the selected organisms.

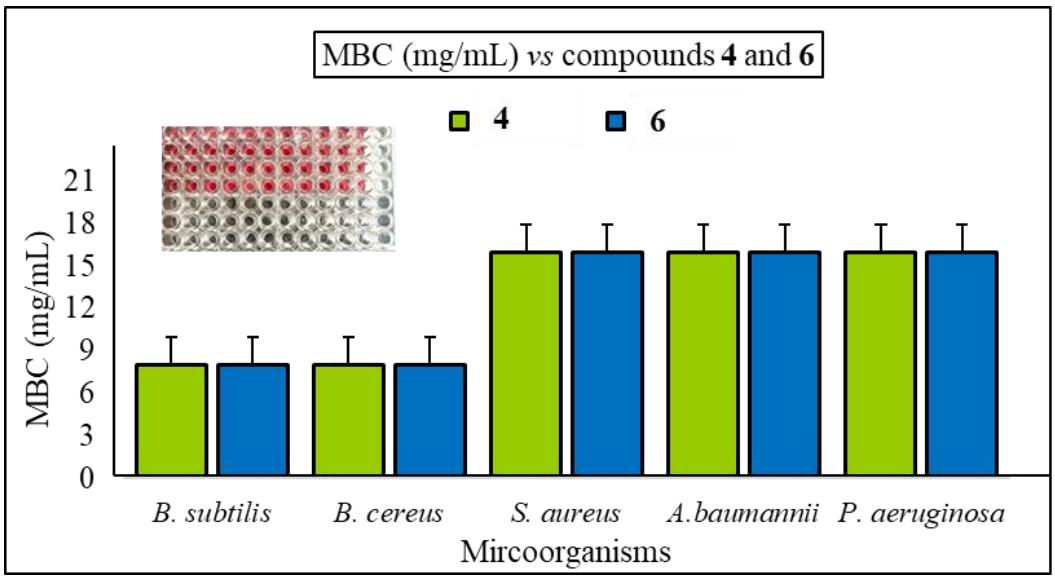

Figure 9. MBC values against the selected organisms.

3.5 Effectiveness of antifungals

Figure 10 shows that most of the MGP derivatives (**2-6**) essentially inhibited the mycelial growth of both *A. niger* and *A. flavus*. With respect to antifungal potential, compound **2** inhibited (77.00±1.0%) *A. flavus*. In the mycelial growth test, remarkable mycelial growth prevention was also observed for compound **3** against *A. niger* (67.71±1.1%) and *A. flavus* (75.45±1.0%). Moreover, promising mycelial growth prevention also occurred for compounds **4** and **5** against *A. flavus* (75.48±1.0% and 77.26±1.0%, respectively) in the mycelial growth test. Furthermore, compound **6** strongly inhibited *A. niger* (76.22±1.1%*)* (**Figure S1**) and *A. flavus* (79.92±1.0%). Compounds **3** and **6** exhibited a greater zone of inhibition than did the conventional antibiotic nystatin when used against *A. niger* and *A. flavus* (**Figure 10**). The incorporation of different acylating groups into the parent compound increased the antifungal activity. The findings showed that the antifungal activity of MGP derivatives **2–6** was markedly increased by the addition of various acyl moieties, such as benzoyl, 2-chlorobenzoyl, 2-bromobenzoyl, and myristoyl groups.[31]

3.6 Antibiofilm activity

Biofilm formation by *Escherichia coli* was prevented by methyl 2,3,4-tri-*O*-myristoyl-6-*O*-heptanoyl-α-D-glucopyranoside (**6**), and the antibiofilm activities of the compounds against *E. coli* were determined to be 8.63, 7.05 and 6.25% at concentrations of 1000, 500 and 250 µg/mL, respectively. **Table 1** shows the optical density values and percentages of biofilm inhibition by various concentrations of compound (**6**).

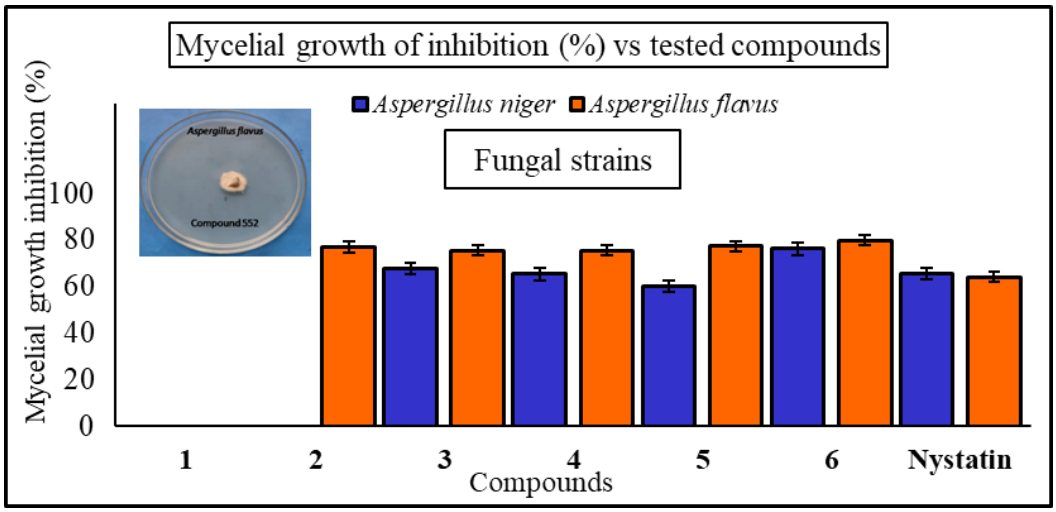

Figure 10. Graph bar for the antifungal activity of the tested MGP derivatives (**2-6**).

Table 1. Antibiofilm activity of compound **6**.

Concentration (µg/mL)	Optical density of control	Optical density of compound 6	Percentage of biofilm inhibition (%)
1000	1.39	1.27	8.63
500	1.39	1.29	7.19
250	1.39	1.30	6.47

The related graphs of the optical density of compound **6**, the optical density of the control and the percentages of inhibition of compound (**6**) against various concentrations of *E. coli* are given below (**Figure 11**).

Several factors are involved in the antibiofilm effect of natural products, including the inhibition of polymer matrix formation, decreased cell adhesion and attachment, interrupted generation of the extracellular matrix (ECM) and reduced production of virulence factors. All these processes result in the blockage of the oxidative stress (OS) network and the development of biofilms.[32] The low efficiency of various antibacterial agents and the *in vivo* toxicity of available antibiotics have driven the discovery of many effective natural antibiofilm agents. Compared with their chemically synthesized counterparts, natural extracts and natural product-based antibiofilm agents are more efficient and have fewer side effects.[33] Like compound **6**, flavonid and saponin glucopyranoside derivatives from *Atriplex tatarica* have been reported to possess antibacterial and antibiofilm activities, whereas apigenin-7-*O*-glucoside also shows similar activity against *Staphylococcus aureus* and *Escherichia coli*.[34]

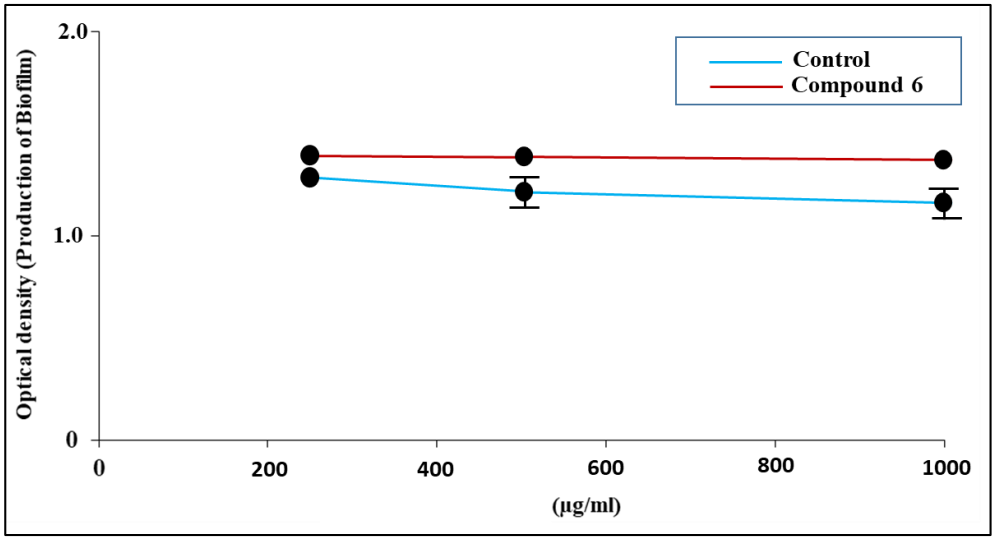

Figure 11. Inhibition of biofilm production by *E. coli* when different concentrations of compound **6** were applied. Biofilm production by the 'control' (in the absence of compound **6**) is shown for comparison. The data are presented as the means ± SDs.

3.7 Structure-activity relationship (SAR)

Antimicrobial development is crucial due to multidrug resistance in common pathogens and emerging diseases. The numerous five- and six-membered heterocyclic compounds that comprise most antimicrobials affect the metabolism of all living cells.[35] The various physiological functions and efficacy of condensed ring structures as favorable therapeutic frameworks have garnered increasing interest. Since glucopyranosides are required for most cellular metabolic functions, they can target enzymes involved in bacterial peptidoglycan, fungal chitin, and protein production. SAR analysis is essential for understanding the antibacterial processes of MGP derivatives. **Figure 12** presents the antimicrobial activities of MGP derivatives, which are readily used to determine the structure-activity relationship (SAR). Since glucopyranoside has a minimal antibacterial effect against pathogenic microbes, structural modifications significantly influence its antibacterial activity. The influence of the following factors clearly decreases in the following order: fused myristoyl>2-chlorobenzoyl for both types of bacteria.

Both compounds **4** and **6** exhibited comparable extents of effectiveness against the tested organisms. Inevitably, it has drawn our attention that-

√ Potential interactions with aliphatic long-chain hydrocarbons

√ The presence of an aromatic ring is crucial for binding

√ Affiliation of the heptanoyl-substituted acyl moiety at position 6 promotes binding interactions

√ The connection of the 2,3,4-substituted acyl component to the myristoyl and 2-Cl. C_6H_4 groups enhance the binding affinity

√ The existence of -Br, -Cl and -CH_3CO- groups in the pyranose ring is also important for the efficacy of the interaction.

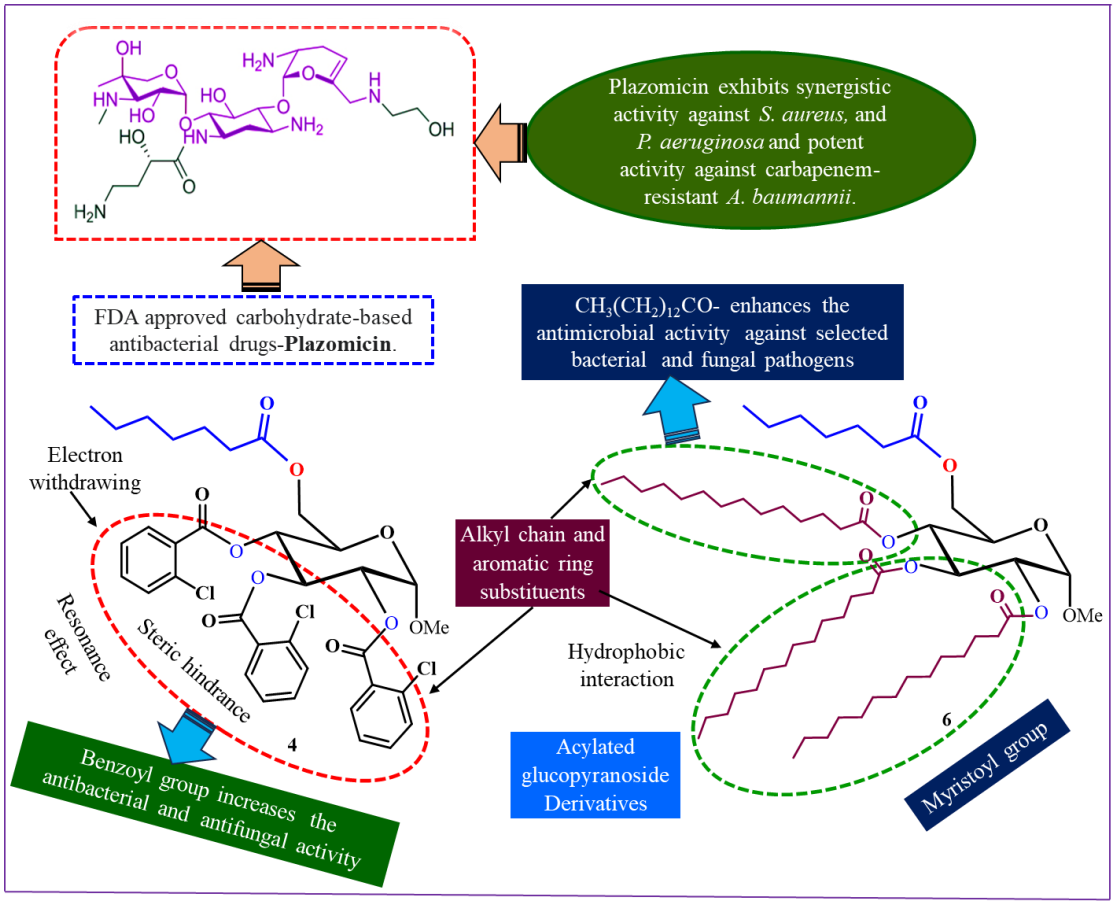

Figure 12. Structure-activity relationship study of the synthesized MGP derivatives.

4. Conclusions

In this work, we designed and synthesized glucopyranoside derivatives that were well characterized by analytical and spectroscopic tools. The incorporation of different aliphatic and aromatic acyl groups into the structure of glucopyranose could greatly enhance its antibacterial activity under testing conditions. The study revealed that the heptanoyl-substituted benzoyl, 2-bromobenzoyl, and myristoyl derivatives **3**, **4** and **6** exhibited greater efficacies against bacterial and fungal strains, along with improved pharmacokinetic and biological profiles. Compound **6** presented significant antibiofilm eradication ability against *E. coli*, which may allow it to be developed as a safe and biocompatible therapeutic agent. Therefore, MGP derivatives are considered to be a significant category of antimicrobial agents that have the potential to be further investigated for their biological and pharmacological features.

Acknowledgments

The authors are grateful to the Research & Publication Office *(Ref.: 946/2022-23/2nd call/04/2023)*, University of Chittagong, Bangladesh for providing

financial support to carry out this piece of research.

Conflicts of Interest

The authors have no conflicts of interest to declare.

Supplementary data

Supplementary data to this article can be found below.

References

1. Finkelstein, J. Glycochemistry & Glycobiology. *Nature*, **2007**, *446*, 999.
2. Persidis, A. The Carbohydrate-Based Drug Industry. *Nat. Biotechnol*., **1997**, *15*, 479–480.
3. Schjoldager, K.T.; Narimatsu, Y.; Joshi, H.J.; Clausen, H. Global View of Human Protein Glycosylation Pathways and Functions. *Nat. Rev. Mol. Cell Biol*., **2020**, *21*, 729–749.
4. McAuliffe, J.C.; Hindsgaul, O. ChemInform Abstract: Carbohydrate Drugs-An Ongoing Challenge. *ChemInform*., **1997**, *28*, 29.
5. Cao, X.; Du, X.; Jiao, H.; An, Q.; Chen, R.; Fang, P.; Wang, J.; Yu, B. Carbohydrate-Based Drugs Launched during 2000−2021. *Acta Pharm. Sin. B.*, **2022**, *12*, 3783–3821.
6. Kawsar, S.M.A.; Matsumoto, R.; Fujii, Y.; Matsuoka, H.; Masuda, N.; Chihiro, I.; Yasumitsu, H.; Kanaly, R.A.; Sugawara, S.; Hosono, M.; Nitta, K.; Ishizaki, N.; Dogasaki, C.; Hamako, J.; Matsui, T.; Ozeki, Y. Cytotoxicity and glycan-binding profile of a D-galactose-binding lectin from the eggs of a Japanese sea hare (*Aplysia kurodai*). *Protein J.,* **2011**. *30*, 509–519.
7. Matsumoto, R.; Fujii, Y.; Kawsar, S.M.A.; Kanaly, R.A.; Yasumitsu, H.; Koide, Y.; Hasan, I.; Iwahara, C.; Ogawa, Y.; Im, C.H.; Sugawara, S.; Hosono, M.; Nitta, K.; Hamako, J.; Matsui, T.; Ozeki, Y. Cytotoxicity and Glycan-Binding Properties of an 18 KDa Lectin Isolated from the Marine Sponge *Halichondria Okadai*. *Toxins*, **2012**, *4*, 323–338.
8. Fujii, Y.; Kawsar, S.M.A.; Matsumoto, R.; Yasumitsu, H.; Ishizaki, N.; Dogasaki, C.; Hosono, M.; Nitta, K.; Hamako, J.; Taei, M.; Ozeki, Y. A D-galactose-binding lectin purified from coronate moon turban, *Turbo (Lunella) coreensis*, with a unique amino acid sequence and the ability to recognize lacto-series glycosphingolipids. *Comp. Biochem. Physiol. Part B: Biochem. Mol. Biol.*, **2011**, *158*, 30**–**37.
9. Kawsar, S.M.A.; Takeuchi, T.; Kasai, K.; Fujii, Y.; Matsumoto, R.; Yasumitsu, H.; Ozeki, Y. Glycan-Binding Profile of a D-Galactose Binding Lectin Purified from the Annelid, Perinereis Nuntia Ver. Vallata, *Comp. Biochem. Physiol. Part B Biochem. Mol. Biol*., **2009**, *152*, 382–389.
10. Kawsar, S.M.A.; Mostafa, G.; Huq, E., Nahar, N.; Ozeki, Y. Chemical Constituents and Hemolytic Activity of *Macrotyloma uniflorum* L., *Int. J. Biol. Chem*., **2009**, *3*, 42–48.
11. Olennikov, D.N.; Tankhaeva, L.M.; Nikolaeva, G.G.; Tsyrenzhapov, A.V.; Nikolaev, S.M.; Chekhirova, G.V. Biologically Active Substances from *Cacalia Hastate* Leaves. 1. Carbohydrates from Leaves and Their

Hypoglycemic Activity, *Chem. Nat. Compd*., **2004**, *40*, 1–5.
12. Kabir, A.K.M.S.; Kawsar, S.M.A.; Bhuiyan, M. Biological Evaluation of Some Mannopyranoside Derivatives, *Bull. Pure Appl. Sci*., **2004**, *23*, 83–91.
13. Misbah, M.M.H.; Ferdous, J.; Bulbul; M.Z.H.;, Dey, S.; Chowdhury, T.S.; Hasan, I.; Kawsar, S.M.A. Evaluation of MIC, MBC, MFC and Anticancer Activities of Acylated Methyl β-D-Galactopyranoside Esters, *Int. J. Biosci*., **2020**, *16*, 299–309.
14. Amin, M.R.; Yasmin, F.; Hosen, M.A.; Dey, S.; Mahmud, S.; Saleh, M.A.; Emran, T.B.; Hasan, I.; Fujii, Y.; Yamada, M.; Ozeki, Y.; Kawsar, S.M.A. Synthesis, Antimicrobial, Anticancer, PASS, Molecular Docking, Molecular Dynamic Simulations & Pharmacokinetic Predictions of Some Methyl β-D-Galactopyranoside Analogs, *Molecules*, **2021**, *26*, 7016.
15. Devi, S.R.; Jesmin, S.; Rahman, M.; Manchur, M.A.; Fujii, Y.; Kanaly, R.A.; Ozeki, Y.; Kawsar, S.M.A. Microbial efficacy and two step synthesis of uridine derivatives with spectral characterization. *ACTA Pharm. Sci.*, **2019**, *57*, 47–68.
16. Kabir, A.K.M.S.; Kawsar, S.M.A.; Bhuiyan, M.M.R.; Rahman, M.S.; Chowdhury, M.E. Antimicrobial Screening of Some Derivatives of Methyl α-D-Glucopyranoside: Antimicrobial Studies of Methyl Gloucopyranoside Derivatives. *Pak. J. Sci. Ind. Res*., **2009**, *52*, 138–142.
17. Bulbul, M.Z.H.; Chowdhury, T.S.; Misbah, M.M.H.; Ferdous, J.; Dey, S.; Hasan, I.; Fujii, Y.; Ozeki, Y.; Kawsar, S.M.A. Synthesis of New Series of Pyrimidine Nucleoside Derivatives Bearing the Acyl Moieties as Potential Antimicrobial Agents. *Pharmacia*., **2021**, *68*, 23–34.
18. Kabir, A.K.M.S.; Kawsar, S.M.A.; Bhuiyan, M.M.R.; Rahman, M.S.; Banu, B. Biological Evaluation of Some Octanoyl Derivatives of Methyl 4,6-*O*-Cyclohexylidene-& Alpha;-D-Glucopyranoside. *Chittagong Univ. J. Biol. Sci*., **2013**, *3*, 53–64.
19. Clinical and Laboratory Standards Institute (CLSI). Methods for Dilution Antimicrobial Susceptibility Tests for Bacteria That Grow Aerobically. 11th ed. CLSI standard M07 (ISBN 1-56238-836-3 [Print]; ISBN 1-56238-837-1 [Electronic]). 950 West Valley Road, Suite 2500, Wayne, Pennsylvania 19087 USA, **2018**.
20. Bauer, A.W.; Kirby, W.M.M.; Sherris, J.C.; Turck, M. Antibiotic Susceptibility Testing by a Standardized Single Disk Method. *Am. J. Clin. Pathol*., **1966**, *45*, 493–496.
21. Hasan, I.; Ozeki, Y.; Kabir, S.R. Purification of a Novel Chitin-Binding Lectin with Antimicrobial and Antibiofilm Activities from a Bangladeshi Cultivar of Potato (*Solanum Tuberosum). Indian J. Biochem. Biophys*., **2014**, *51*, 142–148.
22. Hunt, W.A. The effects of aliphatic alcohols on the biophysical and biochemical correlates of membrane function. *Adv. Exp. Med. Biol*., **1975**, *56*, 195–210.
23. Kim, Y.; Farrah, S.; Baney, R.H. Structure–Antimicrobial Activity Relationship for Silanols, a New Class of Disinfectants, Compared with Alcohols and Phenols. *Int. J. Antimicrob. Agents*, **2007**, *29*, 217-222
24. Akter, N.; Bourougaa, L.; Mebarka, O.; Bhowmic, R.C.; Uddin, K.M.; Bhat, A.R.; Ahmed, S.; Kawsar,

S.M.A. Molecular Docking, ADME-Tox, DFT and Molecular Dynamics Simulation of Butyroyl Glucopyranoside Derivatives against DNA Gyrase Inhibitors as Antimicrobial Agents. *J. Mol. Struct.*, **2024**, *1307*, 137930.
25. Sultana, S.; Hossain, M.A.; Biswas, S.; Saleh, M.A.; Ali, F.; Kawsar, S.M.A. Chemical reactivity, molecular electrostatic potential, FTIR, NMR, in vitro, and in silico studies of mannopyranoside derivatives: 3-Nitrobenzoylation leads to improved antimicrobial activity. *Chem. Phys. Impact.*, **2014**, *9*, 100692.
26. Giri, S.K.; Yadav, N.; Kartha, K.P.R. Acyl transfer reactions on carbohydrates: Peracetylation, an overview. *Trends Carbohydr. Res*., **2015**, *3*, 6–27.
27. Kayes, M.R.; Saha, S.; Alanazi, M.M.; Ozeki, Y.; Pal, D.; Hadda, T.B.; Legssyer, A.; Kawsar, S.M.A. Macromolecules: Synthesis, Antimicrobial, POM Analysis and Computational Approaches of Some Glucoside Derivatives Bearing Acyl Moieties. *Saudi Pharm. J*., **2023**, *31*, 101804.
28. Islam, A.U.; Hadni, H.; Ali, F.; Abuzreda, A.; Kawsar, S.M.A. Synthesis, Antimicrobial Activity, Molecular Docking, Molecular Dynamics Simulation, and ADMET Properties of the Mannopyranoside Derivatives as Antimicrobial Agents. *J. Taibah Univ. Sci*., **2024**, *18*, 2327101.
29. Islam, S.; Hosen, M.A.; Ahmad, S.; ul Qamar, M.T.; Dey, S.; Hasan, I.; Fujii, Y.; Ozeki, Y.; Kawsar, S.M.A. Synthesis, Antimicrobial, Anticancer Activities, PASS Prediction, Molecular Docking, Molecular Dynamics and Pharmacokinetic Studies of Designed Methyl α-D-Glucopyranoside Esters. *J. Mol. Struct*., **2022**, *1260*, 132761.
30. Akter, N.; Saha, S.; Hossain, M.A.; Uddin, K.M.; Bhat, A.R.; Ahmed, S.; Kawsar, S.M.A. Acylated glucopyranosides: FTIR, NMR, FMO, MEP, molecular docking, dynamics simulation, ADMET and antimicrobial activity against bacterial and fungal pathogens. *Chem. Phys. Impact.*, **2014**, *9*, 100700.
31. Islam, A.U.; Serseg, T.; Benarous, K.; Ahmmed, F.; Kawsar, S.M.A. Synthesis, Antimicrobial Activity, Molecular Docking and Pharmacophore Analysis of New Propionyl Mannopyranosides. *J. Mol. Struct*., **2023**, *1292*, 135999.
32. Lu, L.; Hu, W.; Tian, Z.; Yuan, D.; Yi G.; Zhou, Y.; Cheng, Q.; Zhu, J.; Li, M. Developing Natural Products as Potential Anti-Biofilm Agents, *Chin. Med*., **2019**, *14*, 11.
33. Mishra, R.; Panda, A.K.; Mandal, S.D.; Shakeel, M.; Bisht, S.S.; Khan, J. Natural Anti-Biofilm Agents: Strategies to Control Biofilm-Forming Pathogens. *Front. Microbiol*., **2020**, *11*.
34. Pei, Z-J.; Li, C.; Dai, W.; Lou, Z.; Sun, X.; Wang, H.; Khan, A.A.; Wan, C. The Anti-Biofilm Activity and Mechanism of Apigenin-7-*O*-Glucoside Against *Staphylococcus Aureus* and *Escherichia Coli*. *Infect. Drug Resist*., **2023**, *16*, 2129–2140.
35. Saini, M.S.; Kumar, A.; Dwivedi, J.; Singh, R. A Review: Biological Significances of Heterocyclic Compounds. *Int. J. Pharm. Sci. Res*., **2013**, *4*, 66–77.

Supplementary Material

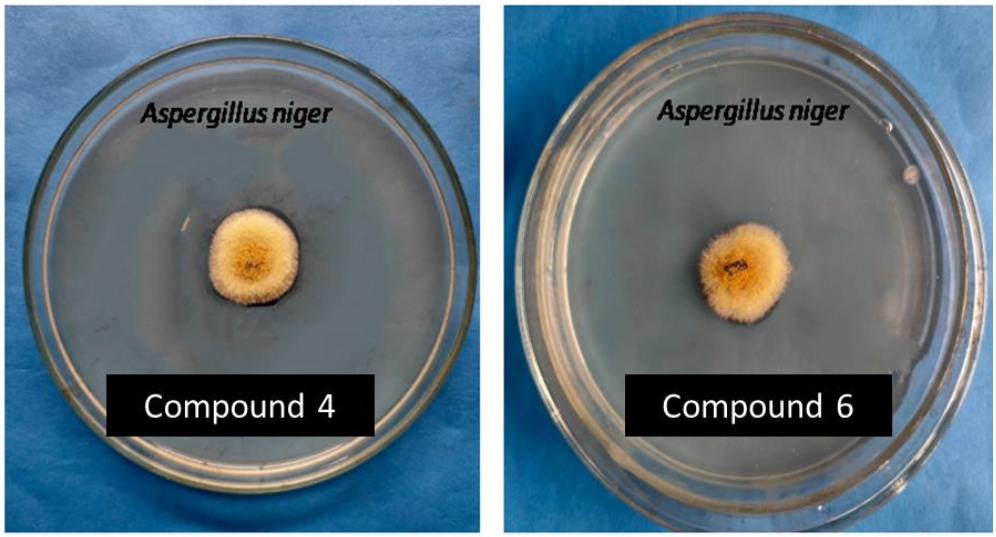

Figure S1. A zone of inhibition was observed against *Aspergillus niger* for compounds **4** and **6**.